# Geometric Reconstruction of the Vascular System of the Rat Brain Imaged by MRA

M. A. Gaudnek[1], A. Hess[2], K. Obermayer[1],
L. Budinsky[3], K. Brune[2,3] and M. Sibila[1]

[1]Neural Information Processing, Faculty IV, Technical University Berlin
[2]Institute for Pharmacology and Toxicology, FAU-Erlangen Nuremberg
[3]Doerenkamp Professor for Innovations in Animal and Consumer Protection

**Abstract.** Functional Magnetic Resonance Imaging (fMRI) would benefit much from high-quality MR Angiography (MRA) of the vascular system underlying the functional domain. Ideally fMRI and MRA are performed during the same experiment. Unfortunately, conventional MRA leads to a systematic underestimation of vessels and images with a generally low contrast. Therefore, we developed a method that combines MRA images from 3 different spatial directions, thus circumventing the most prominent MRA problems. Our method delivers a geometric 3D model of the vessel system that allows visualizations and quantifications beyond the scope of the typically used maximum intensity projections.

## 1 Introduction

Functional Magnetic Resonance Imaging (fMRI) using the blood oxygenation level dependent signal (BOLD) strongly depends on the underlying anatomy of the vascular system [1, 2, 3]. Hereby two parameters are of special importance in their relation to a functional domain, namely i) the vessel diameters and their size distribution and ii) the spatial relation of arteries and veins. One advantage of the non-invasive MRI method is the capability to measure the vascular anatomy by Magnetic Resonance Angiography (MRA) besides measuring fMRI signals in the very same experiment.

Common methods for MRA are the so-called inflow methods [4, 5]. They measure the inflow of pre-saturated blood in a vessel orthogonal to the image plane. Usually axial image planes are taken, because the predominant direction of the blood flow is from anterior to posterior in rodent brains. But this does result in a systematic underestimation of vessels parallel or oblique to this axial image plane.

In this study we try to reconstruct a more complete view of the vascular system by merging the vessels obtained at different imaging planes (axial, sagittal, horizontal). For this purpose we used a snake-based segmentation and non-linear registration algorithms. This approach leads to several advantages. First, a more complete vessel system is obtained which second shows less geometric distortions. Third, by comparing reconstructions of the vascular system before

and after blood pool contrast agent application venous parts of the vascular system can be separated from arterial parts, because contrast agents enhance the venous structures of the vascular system. Moreover, the geometric description of the vascular system easily allows to quantify geometric properties of vessels (position and radius variances, bifurcations, venous-arterial compartments). Again this can be done separately for arteries and veins.

## 2 Methods

### 2.1 Imaging

The imaging is performed on a 4.7 T BRUKER Biospec 47/40 equipped with an actively RF-decoupled coil system. A whole-body birdcage resonator enables homogenous excitation, and a 3 cm surface coil, located directly above the head to maximize the signal-to-noise-ratio, is used as a receiver coil. After dedicated shimming to the imaging volume in order to reduce non-linear image distortions, the angiograms are acquired with a 3D Gradient Echo sequence with a field of view 25×25×25 mm, matrix 256×256×128 pixels, TR = 30 ms, TEef = 3.5 ms, flip angle = 45°, NEX 4). Complete 3D datasets are obtained sequentially at three different orientations viz. axial, sagittal, horizontal. Next, a contrast agent (Endorem 1.2 ml/kg) is applied intravenously and again MRA datasets are recorded.

### 2.2 Segmentation and reconstruction of geometric vascular models

The reconstruction process begins with the separate skeleton reconstruction of each image direction with the method described in [6]. It creates so-called snake models [7] which consist of points characterized by their locations, radii and edges connecting these points, thus spanning 3-dimensional graphs composed of connected frustums, so-called snaxels. The complete graph will be referenced as skeleton from now on.

Reconstruction with this method is a half-automated process which needs the user to set up an initial, very coarse representation of the vessel system, namely starting and ending points of each vessel. All branch points have to be defined before the skeleton is fitted to the data using two methods: i) intensity based fitting, maximizing intensity differences between the voxels contained by the snaxels and those surrounding it and ii) gradient based fitting placing the snaxel boundaries onto the gradients with highest amplitude. Both methods are used simultaneously with adjustable weighting.

### 2.3 Alignment of the different vascular models

The alignment starts with a coarse fitting of the different vascular models which requires at least 3 manually defined landmarks per skeleton. After setting the landmarks a “rubber band algorithm” is applied, i.e. the associated landmarks

**Fig. 1.** Alignment of the black to the white skeleton. Skeleton transformation is achieved by shifting the edges of the surrounding cuboid, $s_{ijk}$ is the shift vector of the cuboid vertex at position (i, j, k). (a) shows the initial cuboid and optimal shift vectors, (b) shows the applied shift vectors resulting in a transformed cuboid which is split into halves for the next iteration imaged in (c).

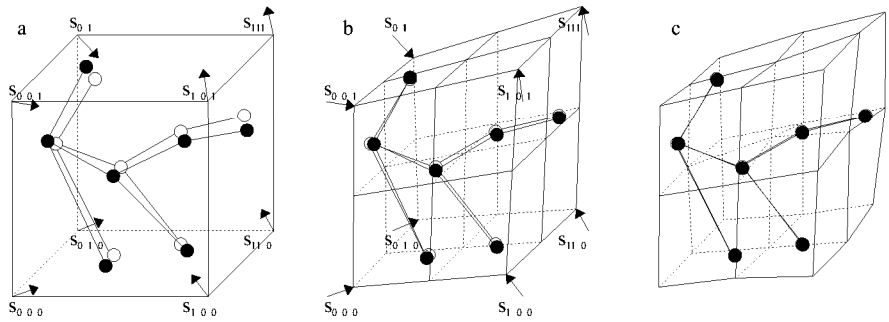


are treated as if rubber bands were spanned between them. This applies forces onto the landmarks which bring them together, thereby pulling the rest of the skeletons with them. The models are rotated and translated until equilibrium of all forces and moments generated by the virtual rubber bands is reached.

The subsequently applied fine alignment consists of an iterative algorithm defining individual transformations for increasingly smaller spatial areas (cuboids). It minimizes an energy function which is the summation of the distances between the points of one skeleton and the nearest neighbours of these points in the other skeletons. The equation for the energy between two skeletons $s$ and $t$ is

$$E_{s,t} = \sum_{p \in P(s)} ||p - n_t(p)|| \tag{1}$$

with $n_t(p)$ being a nearest neighbour of point $p$ in skeleton $t$.

At first the algorithm wraps a separate cuboid around each skeleton to be optimised. Then the skeletons are transformed by shifting the cuboid vertices, dragging the points within the cuboid accordingly. Fig. 1 explains this approach.

In order to minimize the skeleton energy, its change with respect to the modification of the vertex shift vectors has to be inspected. This energy gradient is

$$\nabla_{s_{000}} E_{s,t} = \sum_{p \in P(s)} \frac{p + v(p) - n_t(p)}{||p + v(p) - n_t(p)||} \cdot (1 - p_x)(1 - p_y)(1 - p_z) \tag{2}$$

for shift vector $s_{000}$. The gradients for the other shift vectors are calculated accordingly.

The shift vectors of the vertices are moved along negative energy gradients, thus minimizing the skeleton energies. After reaching a stable state the cuboids are segmented into eight sub cuboids repeating the energy minimization process as shown in Fig. 1c.

**Fig. 2.** (a) Part of the reconstructed axial vascular system in front of the maximum intensity projection of the source image data. The clippings in (b) and (c) show all three skeletons as line plots, skeleton points are displayed as spheres. (b) Zoomed view of a partial area before fine alignment. (c) The same area as shown in (b) after the fine alignment process. The information gained by combining the three skeletons is shown in (d), with grey parts belonging to the reference and black parts belonging to the additional skeletons.

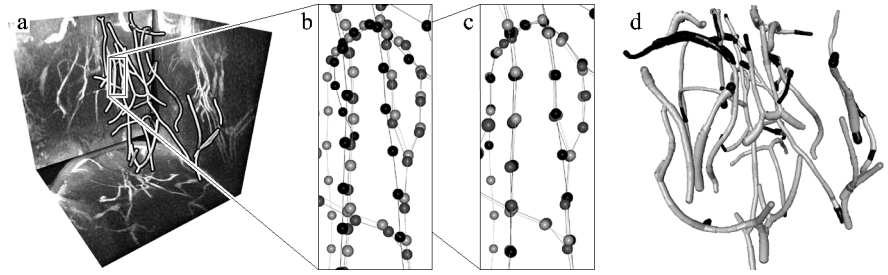


## 3 Results

The reconstruction of the three distinct skeletons from the image volumes (Fig. 2a) and the subsequent coarse alignment already results in a well matching skeleton set (Fig. 2b). However, fine alignment noticeably improves the matching of the three distinct models (Fig. 2c). For the skeleton shown in Fig. 2 the average distance between nearest neighbours was reduced from 1.36 to 0.47 voxels for the sagittal and from 1.57 to 0.68 voxels for the horizontal skeleton. The remaining distances between the skeletons are at almost every location far below the snaxel diameters, so correct assignment of the skeleton parts for adjacent skeleton merging is ensured.

The amount of information that can be retrieved from the geometric 3D reconstruction is superior compared to that retrievable by just inspecting the maximum intensity projections of the image data (cf. Fig. 2a). Once the snake model of the vascular system is extracted, it can easily be visualized from any direction.

As already described using three imaging directions allows to extract significant more parts of the vascular system than only one imaging direction would allow. This information gain of vascular components is illustrated in Fig. 2d.

## 4 Discussion and Outlook

In this study we showed that already the half-automated reconstruction of the geometric structure of vascular systems results in representations of the vascular system that offer superior examination capabilities compared to the commonly used maximum intensity projections. By incorporating three orthogonal imaged data sets we were able to create models that obtain significantly more details

than those resulting from only one image direction. Moreover, the overall geometric distortions among them are reduced after fusing the different reconstructions.

The next steps will further increase the degree of automation. Currently the different modules still need manual adjustment influencing the reconstruction behaviour and consequently the reconstruction quality. In the future automatic presetting will assist the user in finding good parameters. Strong increase in automation is also planned for the final merging of the skeletons to one common model, which will be performed by a full automatic graph matching algorithm.

First results already show that by the described approach arteries can be differentiated from veins and examined separately. Encouraged by our previous results we will try to fuse the reconstructed vessel system with functional imaging data of the very same specimen in our future research. This will allow a more detailed analysis of the commonly used fMRI BOLD signal.

## References

1. Hess A, Stiller D, Kaulisch T, et al. New insights into the hemodynamic blood oxygenation level-dependent response through combination of functional magnetic resonance imaging and optical recording in gerbil barrel cortex. J Neurosci 2000;20(9):3328–3338.
2. Logothetis NK, Wandell BA. Interpreting the BOLD Signal. Annu Rev Physiol 2004;66:735–769.
3. Matthews PM, Jezzard P. Functional Magnetic Resonance Imaging. J Neurol Neurosurg Psychiatry 2004;75(1):6–12.
4. Hilger T, Niessen F, Diedenhofen M, et al. Magnetic Resonance Angiography of Thromboembolic Stroke in Rats: Indicator of Recanalization Probability and Tissue Survival After Recombinant Tissue Plasminogen Activator Treatment. J Cereb Blood Flow Metab 2002;22(6):652–662.
5. Reese T, Bochelen D, Sauter A, et al. Magnetic Resonance Angiography of the Rat Cerebrovascular System Without the Use of Contrast Agents. NMR Biomed 1999;12(4):189–196.
6. Schmitt S, Evers JF, Duch C, et al. New Methods for the Computer-Assisted 3D Reconstruction of Neurons from Confocal Image Stacks. Neuroimage 2004;23(4).
7. Kass M, Witkin A, Terzopoulos D. Snakes: Active Contour Models. Int J Computer Vision 1987;1(4):321–331.